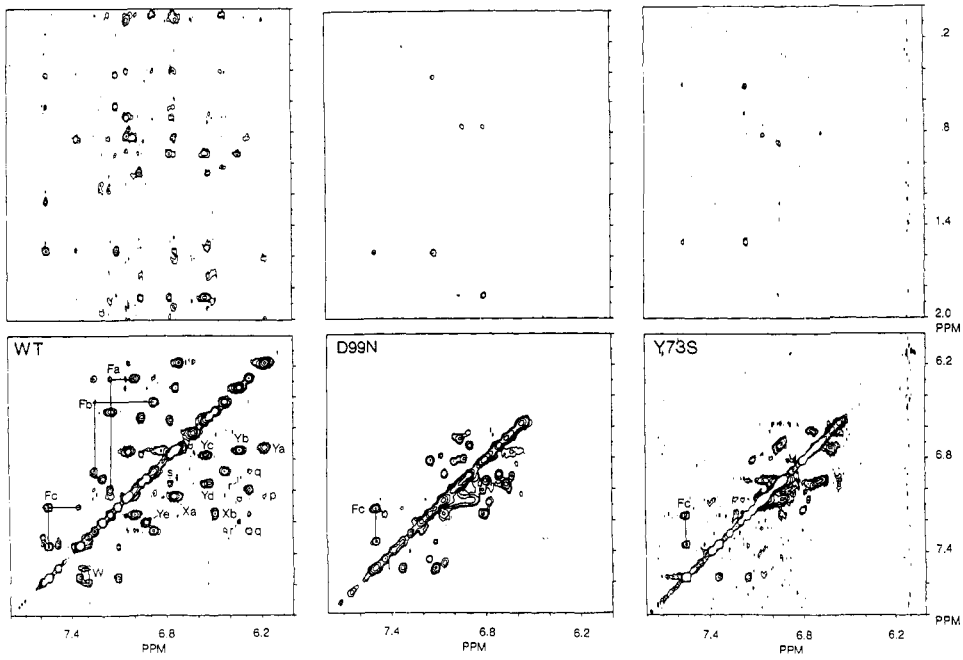

Figure 2. Phase-sensitive NOESY spectra of WT, D99N, and Y73S in D_2O at 500 MHz. The sample conditions are the same as in Figure 1. The mixing time was 200 ms. A 4096 × 512 matrix in the time domain was recorded and zero-filled to a 4096 × 2048 matrix prior to multiplication by a Gaussian function (LB −3, GB 0.1). Although the proton resonances of *porcine* PLA2 have been assigned completely,[14] only limited spin systems have been assigned for the *bovine* enzyme.[12,15] The letters F, Y, and W represent Phe, Tyr, and Trp, respectively, while X is uncertain. The small letters p–s designate interresidue NOE cross peaks.

and Y73S, respectively), suggesting substantial decreases in the conformational stability of the mutant PLA2s. However, the fact that the mutants can still undergo cooperative denaturation distinguish them from real molten globules.[7b,c]

It is striking that both Tyr-73 and Asp-99 are part of the conserved "catalytic network"[9,10] at the active site; the two side chains are connected by a hydrogen bond, and Asp-99 is further H-bonded to the general base His-48. It is even more striking that the highly flexible mutants are still functional, though with activities diminished 10–100-fold.[11,12] Although the latter is expected for active site mutants, our results only allow us to conclude that the two residues play critical structural roles; their functional roles remain to be established.

One should not be led to think that the structure of PLA2 is "fragile". None of the site-specific mutations at seven other conserved positions (Tyr-52, Lys-53, Lys-56, Phe-22, Phe-106, Cys-51, and Cys-98) resulted in large structural perturbations. The Y52V (Tyr-52 is also H-bonded to Asp-99) PLA2 showed activity similar to Y73S, but strikingly similar NOESY spectra relative to the WT enzyme.[12] The double mutant C51A/C98A, in which a disulfide bond has been deleted, exhibited normal activity and only a modest decrease in $\Delta G_d^{H_2O}$ (7.2 kcal/mol). Site-specific substitutions of Phe-22 (to Ile and Ala) and Phe-106 (to Ile, Ala, and Tyr), which were involved in three-way aromatic–aromatic interactions along with Phe-5 in the crystal structure,[9,13] resulted in only small and localized changes in NOESY spectra.

The disappearance of NOEs could be caused by either decreased τ_c (such that $\omega_0\tau_c \approx 1$) or increased average internuclear distances. Other approaches are being undertaken to differentiate these possibilities, to uncover structural basis for the observed effects, and to determine if the conformations are induced back upon binding to micelles.

(9) Dijkstra, B. W.; Kalk, K. H.; Hol, W. G. J.; Drenth, J. *J. Mol. Biol.* **1981**, *147*, 97–123.
(10) Brunie, S.; Bolin, J.; Gewirth, D.; Sigler, P. B. *J. Biol. Chem.* **1985**, *260*, 9742–9749.
(11) Dupureur, C. M.; Deng, T.; Kwak, J.-G.; Noel, J. P.; Tsai, M.-D. *J. Am. Chem. Soc.* **1990**, *112*, 7074–7076.
(12) Dupureur, C. M.; Yu, B.-Z., Jain, M. K.; Noel, J. P.; Deng, T.; Li, Y.; Byeon, I.-J. L.; Tsai, M.-D., submitted for publication.
(13) Noel, J. P.; Bingman, C. A.; Deng, T.; Dupureur, C. M.; Hamilton, K. J.; Jiang, R. T.; Kwak, J.-G.; Sekharudu, C.; Sundaralingam, M.; Tsai, M.-D. *Biochemistry* **1991**, *30*, 11801–11811.
(14) Dekker, N.; Peters, A. R.; Slotboom, A. J.; Boelens, R.; Kaptein, R.; de Haas, G. *Biochemistry* **1991**, *30*, 3135–3147.
(15) Fisher, J.; Primrose, W. U.; Roberts, G. C. K.; Dekker, N.; Boelens, R.; Kaptein, R.; Slotboom, A. J. *Biochemistry* **1989**, *28*, 5939–5946.

Radical Scavenging in Zeolite Media

M. A. Garcia-Garibay, X. G. Lei, and N. J. Turro*

Department of Chemistry, Columbia University
New York, New York 10025

Received December 11, 1991

The model of the solvent cage predicts that the dynamics of dissociating particles in fluid media depends on their probabilities of escape and recombination[1,2] and that there may be at least three potentially observable stages at which scavenging may occur: (a) primary geminate pairs, (b) secondary geminate pairs, and (c) free radicals.[3]

Experimental tests[3,4] have demonstrated scavenging at stages b and c. However, because of the restricted time resolution available within the dynamics of fluid systems, distinctive scavenging at each intermediate stage has not proven possible.[4] The general concepts of cage effects in liquids have been applied to the dynamic properties of organized media and constrained environments.[5] In this communication, we report an example where

(1) Rabinowitch, E.; Wood, W. C. *Trans. Faraday Soc.* **1936**, *32*, 1381. (b) Franck, J.; Rabinowitch, E. *Trans. Faraday Soc.* **1934**, *30*, 120.
(2) (a) Noyes, R. M. *J. Am. Chem. Soc.* **1955**, *77*, 2042. (b) Noyes, R. M. *Prog. React. Kinet.* **1961**, *1*, 129.
(3) (a) Koening, T. In *Free Radicals*; Kochi, J. K., Ed.; John Wiley: New York, 1973; Vol. 2, Chapter 4, pp 157–163. (b) Khudyakov, I. V.; Yakobson, B. I. *Zh. Obs. Khim.* **1984**, *54*, 3; *J. Gen. Chem. USSR (Engl. Transl.)* **1984**, 1. (c) Eisenthal, K. B. *Acc. Chem. Res.* **1975**, *8*, 118.
(4) For examples that clearly distinguish the trapping of geminate pairs and free radicals, see: (a) Hammond, G. S.; Waits, H. P. *J. Am. Chem. Soc.* **1964**, *86*, 1911. (b) Wu, C.-H. S.; Hammond, G. S.; Wright, J. M. *J. Am. Chem. Soc.* **1960**, *82*, 538.

0002-7863/92/1514-2749$03.00/0 © 1992 American Chemical Society

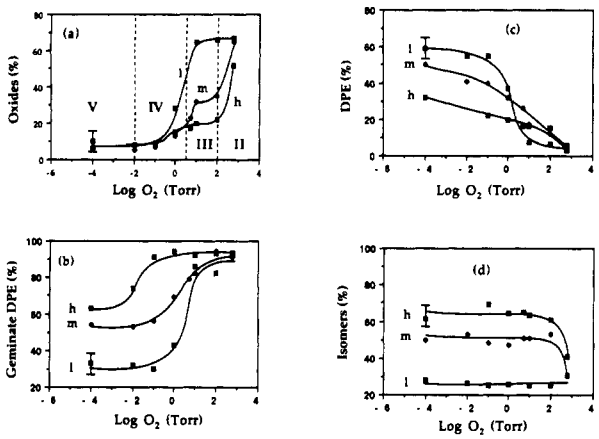

Figure 1. Normalized yields (the sum of all product GLC yields is taken as 100%) of oxides (a), diphenylethane (c), and isomeric (d) products from photolysis of DBK in zeolite NaX at different oxygen pressures and ketone loading values: $\langle S \rangle$ = 0.16 (l), 0.48 (m), and 0.64 (h) molecules per supercage. The percentage of geminate recombination of the Bz••Bz radical pair giving DPE-d_5 is plotted in b.[12]

Scheme I

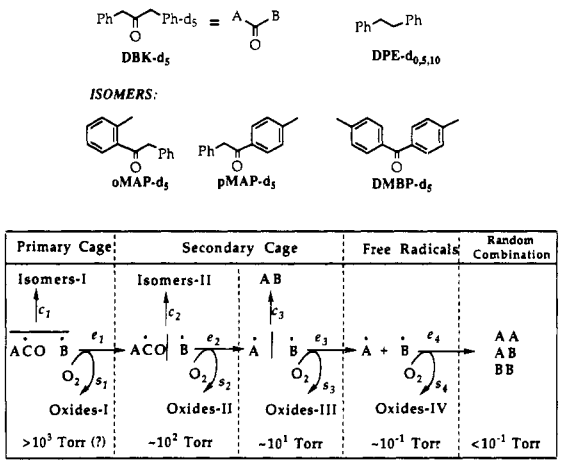

distinctive scavenging at three intermediate stages can be observed by fine-tuning the recombination and escape probabilities of radical pairs in the zeolite NaX.[6]

Radical pairs were generated from the photocleavage of dibenzyl ketone-d_5 (DBK-d_5) with molecular oxygen as the scavenger. Photolysis experiments were carried out with three different loadings of DBK-d_5 and eight different oxygen pressure values (Figure 1a–d). Product mixtures were found to contain DPE-(d_0, d_5, d_{10}), *o*-MAP-d_5, and *p*-MAP-d_5 and the scavenging products (heretofore referred to as oxidation products) benzaldehyde, benzoic acid, and phenylacetic acid (Scheme I).[7,8]

The results in Figure 1 are analyzed conceptually (but not in detail) in terms of Noyes' model[2] as shown in Scheme I. The dynamics of the particles includes three basic steps: escape (e_n), combination (c_n), and scavenging (s_n), which occur in sequential stages (n). The primary cage is the site where a geminate radical pair is created (a zeolite supercage).[9] Escape of a radical to neighboring sites followed by a geminate re-encounter constitutes a secondary cage. Finally, randomization of radical pairs into the zeolite network generates free radicals which terminate by random encounters and combinations. Two consecutive geminate radical pairs of different composition are involved in our system: the primary geminate radical pair (ACO••B) and the secondary geminate radical pair (A••B) resulting from decarbonylation. While the formation of the secondary radical pair could occur in the primary or secondary cages or even after randomization of the pair, our investigations indicate that the conversion of ACO••B into A••B in zeolite NaX occurs at the second stage, as indicated in Scheme I.[6,10]

In the absence of oxygen, evolution of the radical intermediates depends on the rates of escape (e) and combination (c). In the zeolite lattice, the former are determined by the percolation of the radicals through the unoccupied supercage network and depend on the amount of DBK (loading level) in the system.[6] The effect of oxygen as a scavenger will depend on its concentration and its ability to intercept intermediates before escape to the next level occurs.

Scavenging of Free Radicals. The three lines in Figure 1a–d (l, m, and h) refer to (*l*ow, *m*edium, *h*igh) loading values $\langle S \rangle$ of 0.16, 0.48, and 0.64, where $\langle S \rangle$ is the number of molecules per supercage. The yields of oxidation products (P_{ox}) are shown as a function of oxygen pressure for the three different loadings. Different scavenging regimes with labels corresponding to those in Scheme I are indicated in Figure 1a. A region of constant (static) scavenging with yields of ca. 7% was found for all three loadings between pressures of 10^{-4} and 10^{-2} Torr due to reaction with chemisorbed oxygen (Oxides-V).[11] The profiles of Figure 1a are different for samples with different substrate loadings. While curve l presents a single step between two constant regimes, curves m and h present up to three distinct scavenging domains (Oxides-II to -IV). The first scavenging step (at $\sim 10^{-1}$ Torr O_2) in the curves of Figure 1a monitors the interception of free radicals (i.e., e_4 vs s_4) giving rise to benzaldehyde and benzoic acid (i.e., Oxides-IV). This results in an increase in the fraction of secondary geminate pairs undergoing combination [percentage of geminate DPE (DPE-d_5) in Figure 1b] and a decrease of the total yields of DPE by scavenging of the radicals undergoing random encounters (Figure 1c).[12] The amplitude of the first step in the curves in Figure 1a reflects the fraction of geminate pairs that ultimately become free radicals (ca. 0.5 at $\langle S \rangle$ = 0.16 and ca. 0.1 at $\langle S \rangle$ = 0.48 and $\langle S \rangle$ = 0.64). The experimental uncertainty in the first scavenging step of curves m and h in Figure 1a is largely reduced in Figure 1b where the percentage of geminate DPE remaining also reflects the fraction of free radicals scavenged.

Scavenging of Secondary Geminate Radical Pairs. An increase in the amount of oxygen results in the onset of a competition of scavenging with recombination and reaction of the secondary radical pair [e_3 vs s_3: Oxides-III, Scheme I]. Oxidation products at this step consist of benzaldehyde and benzoic acid. Scavenging in the global environment of interconnected supercages is manifested both in terms of decreased yields of DPE and increased yields of P_{ox}. However, in this region, little effect is observed in the yields of isomeric products ($e_1 \gg s_1$ and $e_2 \gg s_2$). The fractions of radicals scavenged at this stage from Figure 1a,c are ca. 0.1 and 0.05 at $\langle S \rangle$ = 0.48 and 0.64, respectively.

Scavenging of the Primary Geminate Radical Pair. Combination of the primary radical pair in the secondary cages yields isomeric

(5) (a) Lebedev, Y. S. *Sov. Sci. Rev., Sect. B* **1988**, *11*, 69. (b) Lei, X. *Res. Chem. Intermed.* **1991**, *14*, 15.

(6) Garcia-Garibay, M. A.; Zhang, Z.; Turro, N. J. *J. Am. Chem. Soc.* **1991**, *113*, 6212.

(7) Experimental details regarding sample preparation and analysis are given in ref 6. Even though the GC analysis conditions were optimized to detect scavenging products, we observed that quantification of their total yields (reported as "oxides") appeared to be more reliable than their individual contributions. *p,p'*-Dimethylbenzophenone (DMBP-d_5) was observed to be a product from secondary photolysis of *p*-MAP at high conversion values.

(8) Samples analyzed by EPR before and after irradiation showed the formation of signals due to unidentified radicals which were shown to be stable over more than 24 h and to disappear in the presence of oxygen. However, their concentration (ca. 2×10^{-7} mol/g) is 3 orders of magnitude too small to represent any sizable fraction of the products discussed in our analysis. We are currently investigating the nature of this species.

(9) Breck, D. W. *Molecular Sieves*; Wiley: New York, 1974.

(10) We have not considered decarbonylation of the primary radical pair in the present system, although it is known to occur in other restricted environments such as in crystalline cyclodextrin complexes: Rao, N. B.; Syamala, M. S.; Turro, N. J.; Ramamurthy, V. *J. Org. Chem.* **1987**, *52*, 5517.

(11) Suib, S. L.; Morse, B. E. *Langmuir* **1989**, *5*, 1340.

(12) The percentage of geminate recombination of the Bz••Bz-d_5 radical pair reported in Figure 1c is generally reported as the "cage effect". This was evaluated by measuring the yields of DPE, DPE-d_5, and DPE-d_{10} by combined GC–MS analyses and applying the formula CE % = [DPE-d_5 − (DPE + DPE-d_{10})]/(DPE + DPE-d_5 + DPE-d_{10}).

products with a p-MAP/o-MAP = 0.3 ratio (Isomers II). We have proposed that these products are formed from radicals escaping the primary cage but that are unable to percolate through the lattice and are forced to reencounter. The lifetime of this pair is determined either by decarbonylation (e_2) or by reencounter and reaction (c_2, Scheme I), and the largest scavenging effects are observed on the yield of isomerization products and on the yields of oxides, which include the formation of phenylacetic acid (Oxides-II). The amplitude between the last two points in lines m and h of Figure 1a,d at pressures approaching 10^3 Torr reflects the fraction of radicals involved at this stage. Finally, at the end of the scavenging dynamics is the primary radical pair in the primary cage. The nonscavenging products remaining at high pressures (Isomers-I) come from reactions at the primary geminate site (supercage) and are characterized by p-MAP/o-MAP $\approx$ 0.15 with $\langle S \rangle$ = 0.64 and 0.48 at the highest oxygen pressures.

Although the dynamics of the radical pairs produced from photolysis of DBK in solution basically occurs in a succession of unresolvable steps, the conditions for time management in complex chemical and molecular dynamics not available in fluid media may be found in organized media such as zeolites.

Acknowledgment. The authors acknowledge the NSF, AFOSR, and DOE for their generous support of this research.

Experimental and Theoretical Evidence in Support of an Intermediate Complex in the Insertion Reaction of Silylene into Silane

R. Becerra

Instituto de Quimica-Fisica Rocasolano C. S. I. C., 28006 Madrid, Spain

H. M. Frey, B. P. Mason, and R. Walsh*

Department of Chemistry, University of Reading Whiteknights, P.O. Box 224, Reading RG6 2AD, UK

M. S. Gordon

Department of Chemistry, North Dakota State University, Fargo, North Dakota 58105

Received December 11, 1991

The reaction between silylene, SiH_2, and silane, SiH_4, viz.

$$SiH_2 + SiH_4 \rightarrow Si_2H_6 \quad (1)$$

may reasonably be considered the prototype Si–H insertion process of silicon hydride chemistry. This reaction, which is also the second step in the thermolysis of silane[1] leading ultimately to solid silicon and silicon hydride deposition, is known to be fast. Experimental measurements of the rate constant[2-4] show the reaction to proceed at close to the collisional limit. Theoretical calculations of the energy surface for the decomposition of Si_2H_6 show that it possesses no energy barrier at the threshold of dissociation,[5] which suggests a zero barrier for reaction 1. The published kinetic studies of reaction 1[2-4] have only been carried out at room temperature. We present here new experimental rate measurements of reaction 1 in the gas phase over the temperature range 296–658 K, supported by ab initio calculations which provide unambiguous evidence for a barrierless reaction and additionally suggest the existence of a weakly bound complex in the reaction potential entrance channel.

Table I. Experimental Rate Constants for Reaction 1 at Different Temperatures (Bath Gas SF_6)

T/K	$10^{10}k$/cm^3 molecule^{-1} s^{-1} P = 10 Torr	$P = \infty$[a]
296	4.2	4.6 ± 0.3
363	3.3	3.9 ± 0.3
432	2.9	3.2 ± 0.3
488	1.90	2.6 ± 0.3
578	1.28	2.6 ± 0.4
658	0.72	2.2 ± 0.4

[a] Obtained by extrapolation.

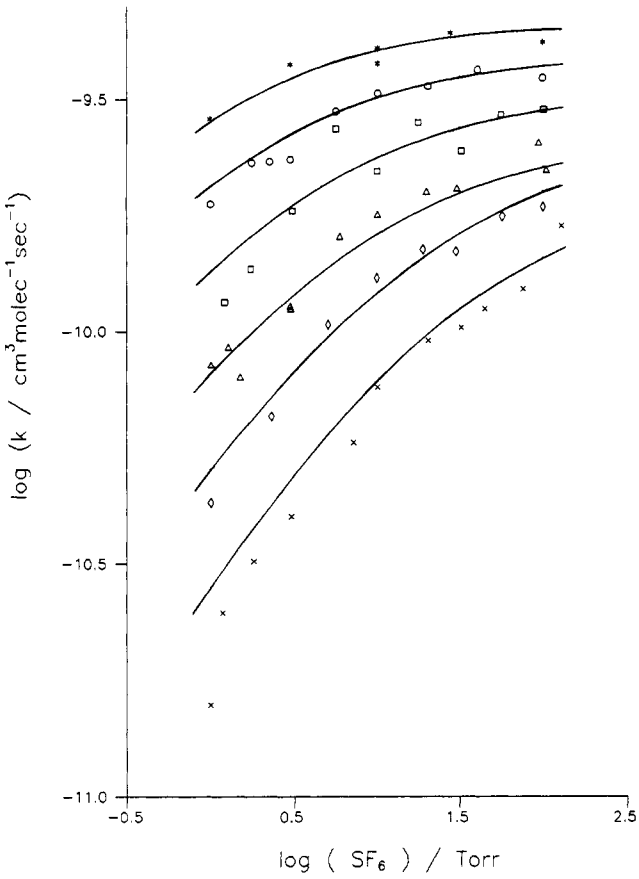

Figure 1. Pressure dependence of second-order rate constants for reaction 1 at different temperatures [*, 296 K; ○, 363 K; □, 432 K; △, 488 K; ◇, 578 K; ×, 658 K]. Solid lines are variational RRKM theoretical fits.

SiH_2 kinetic studies have been carried out by the laser flash photolysis technique, the details of which have been published previously.[4,6] SiH_2 was created by photodecomposition of phenylsilane using the 193-nm ArF line of a pulsed excimer laser. SiH_2 was detected and monitored in real time by use of a single-mode dye laser tuned to a known (strong) vibration–rotation transition (17259.50 cm^{-1}) in the visible A ← X absorption band. Signal decays from 5–15 photolysis laser shots were averaged and found to give good first-order kinetic fits. Experiments were carried out with gas mixtures containing a few millitorr of phenylsilane, varying quantities of SiH_4 up to 100 mTorr, and inert diluent bath gas (SF_6 or Ar) at total pressures between 1 and 100 Torr. Second-order kinetics was confirmed by finding a linear pressure dependence of the pseudo-first-order decay constants on substrate SiH_4 pressures.

The reaction was studied at six temperatures in the range 298–653 K. Second-order rate constants were found to be pressure

(1) (a) Purnell, J. H.; Walsh, R. *Proc. R. Soc. London A* **1966**, *293*, 543. (b) Neudorfl, P.; Johdan, A.; Strausz, O. P. *J. Phys. Chem.* **1980**, *84*, 338. (c) White, R. T.; Espino-Rios, R. L.; Rogers, D. S.; Ring, M. A.; O'Neal, H. E. *Int. J. Chem. Kinet.* **1985**, *17*, 338.
(2) Inoue, G.; Suzuki, M. *Chem. Phys. Lett.* **1985**, *122*, 361.
(3) Jasinski, J. M.; Chu, J. O. *J. Chem. Phys.* **1988**, *88*, 1678.
(4) Baggott, J. E.; Frey, H. M.; Lightfoot, P. D.; Walsh, R.; Watts, I. M. *J. Chem. Soc., Faraday Trans.* **1990**, *86*, 27.
(5) (a) Gordon, M. S.; Truong, T. N.; Bonderson, E. K. *J. Am. Chem. Soc.* **1986**, *108*, 2191. (b) Gordon, M. S.; Gano, D. R. *J. Am. Chem. Soc.* **1984**, *106*, 5421.
(6) Baggott, J. E.; Frey, H. M.; King, K. D.; Lightfoot, P. D.; Walsh, R.; Watts, I. M. *J. Phys. Chem.* **1988**, *92*, 4025.

0002-7863/92/1514-2751$03.00/0 © 1992 American Chemical Society